eJNDT e-Journal of Nondestructive Testing - ISSN 1435-4934 - www.ndt.net

EWGAE 2024
36th Conference of the European Working Group on Acoustic Emission

The capability of Acoustic Emission Features to monitor Diamond-Coated Burr grinding wear and effectiveness

Thomas JESSEL [1], Carl BYRNE [1], Mark EATON [1] and Rhys PULLIN [1]

[1]Cardiff School of Engineering, Cardiff University, Cardiff, UK
jesselt@cardiff.ac.uk, byrne@cardiff.ac.uk, eatonm@cardiff.ac.uk, pullinr@cardiff.ac.uk

Abstract. Within manufacturing there is a growing need for autonomous Tool Condition Monitoring (TCM) systems, with the ability to predict tool wear and failure. This need is increased, when using specialised tools such as Diamond-Coated Burrs (DCBs) for mill-grinding high strength ceramics or glass, in which the random nature of the tool, inconsistent manufacturing methods and high wear rates create large variance in tool life. This unpredictable nature leads to a significant fraction of a DCB tool's life being underutilised due to premature replacement. Workpiece surface damage, increased grinding forces and large-scale diamond grain pullout could all be the result of high levels of runout and in-circularity common within electroplated DCBs. As such it is important to not only monitor the overall tool wear but also tool condition. Acoustic Emission (AE) presents as an indirect on-machine sensing method highly suited to grinding applications. The high frequency range of AE, >20 kHz, prevents machine noise from dominating the acquired signals, isolating the microscale machining processes within noisy machine environments. AE resulting from the grinding process has the potential to monitor not only tool wear but also key performance indicators of a tools condition. A series of DCB mill-grinding tests have been conducted, each consisting of the continuous acquisition of AE during grinding. In addition a complimentary data set of frequent tool surface measurements was acquired to support AE analysis. Preliminary results demonstrate AE kurtosis can be seen as an indicator of each tool's runout, representing the fraction of time the tool and workpiece are in contact during a revolution. As a result, an indirect monitoring system capable of monitoring wear and tool state with AE could be utilised within the manufacturing sector.
Keywords: Acoustic Emission, Tool Condition Monitoring, Diamond Coated Burrs, Grinding

Introduction

The increasing demand for higher strength materials within mass-manufacturing has led to the dramatic increase in use of small diameter grinding tools. Of which, electroplated single-layer Diamond-Coated Burrs (DCBs) are common-place, enabling small and complex, ceramic or glass components to be manufactured. This widespread use stems from the electroplating manufacturing method, allowing DCBs to take on any required geometric profile with little additional expense. However, the electroplating method is also the main

https://doi.org/10.58286/30231

downside of these tools. Electroplated DCBs are mono-layer grinding tools, in which a single layer of diamond grains are plated onto the tool's core, with a nickel bond material. Fig. 1 shows the circumferential cross-section of a ⌀ 1.3 mm #1000 (15 µm grain size) DCB, in which you can see the tool's steel core and the diamond grains encased by the nickel plating.

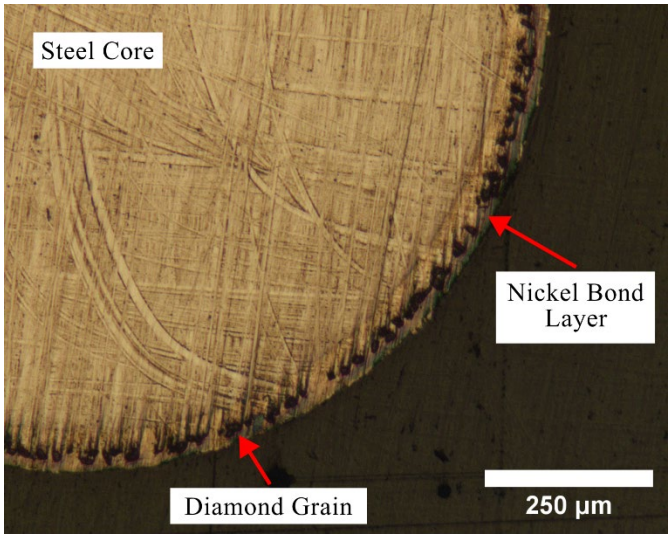

Fig. 1. Radial cross-section of a new ⌀ 1.3 mm #1000 DCB

The random nature of electroplating results in defects on the tool surface, including nickel blisters, uneven grit density, flat spots, and high levels of runout/ovality. The outcome of these inconsistencies/defects are tools with inherently different Remaining Usable Life (RUL). With the current time based tool life management strategy, it is typical for only 50–80% of a DCBs' life to be utilised [1] before being replaced. Furthermore, 20% of a machine tool's downtime is the direct result of tool failure [2].

Utilised as "mill-grinding" tools, DCBs exhibit similar characteristics of both grinding wheels and end mills. Grinding tool wear results from the cumulation of many individual rotational interactions between abrasive grains and the workpiece material [3]. The outcome of these interactions can be separated into three main mechanisms of wear: attritous wear, micro/macro grain fracture and bond fracture [4]. The monitoring of these tools however is lacking in comparison to other traditional machine processes, such as milling and turning. As such, a passive sensing process that could allow for on-machine real-time monitoring would be highly beneficial, resulting in reducing tooling costs and machine downtime.

Indirect Tool Condition Monitoring (TCM) methods whilst less precise than direct optical or physical measurements, are still beneficial within mass-manufacturing due to their uninterrupted nature [5]. In an attempt to fill this void, Acoustic Emission (AE) was utilised as an indirect sensing technique. AE is already deployed as a promising and widely used method for grinding process monitoring, including the dressing process [6, 7], wheel loading [8, 9] and grinding burn [10, 11]. Additionally, the ultrasonic nature of AE waveforms, >20 kHz, prevents machine noise from dominating the acquired signals [12, 13]. This built-in filtering effect allows for a high signal/noise ratio and sensitivity at the micro scale encountered from extremely small depth of cuts [14, 15]. In order to prevent attenuation of the higher frequency components, AE sensors are typically mounted directly to the workpiece [16, 17], reducing the distance between the source and sensor face. Other studies have been carried out in attempt to remove this limitation, such as mounting to the work-holding device [11, 18], spindle head [19, 20] or through the coolant flow [21, 22].

This paper presents the results from four mill-grinding tests, during each a DCB was worn systematically with frequent direct surface measurements. AE was collected during each grinding pass throughout the tool's life, allowing for a TCM approach to be developed based solely on AE. A Renishaw NC4 system [23] was utilised to directly measure the tool's surface from within the machine tool, from which the tool wear and condition could be monitored throughout. AE showed the ability to identify the grinding contact period and as a result automatic trigger points were determined, focusing AE features on this period. AE Kurtosis (AE_{kurt}), a measure of a distribution's peakedness and an indicator for fault diagnosis of rotating machinery [24], was identified as a useful feature to relate AE to the tool's condition, seen by both runout and form error. Potentially, allowing future TCM models to predict a combination of both overall wear, tool radius, and grinding effectiveness, runout and form error.

1. Methodology

This section outlines the experimental procedure for the grinding procedure and AE acquisition. For a more detailed description of the methodology the reader is referred to a previous publication on this work [25].

Four tool life tests were carried out, all of which utilised the same procedure, grinding parameters, data acquisition setup and tool specification. Each test started with an un-used Genentech ⌀ 1.3mm #1000 (15 μm average grain size) DCB, and was used to grind a silicon carbide workpiece until tool failure.

A MISTRAS Wideband Differential (WD) sensor was used in conjunction with a MISTRAS 2/4/6 pre-amplifier, set to a gain of 20 dB. The WD sensor was coupled directly to the top surface of the workpiece, with a setting silicon based sealant to prevent water ingress and act as a couplant between the two surfaces. A National Instruments PXI-5922 oscilloscope was used to record the AE signals at 2 MHz.

To wear the DCBs a single side-grinding pass was repeated until tool failure, deemed by a reduction of >0.5 mm in the tool's length, grinding parameters can be found in detail in [25]. After each grinding pass the DCB's surface was measured halfway up the axial depth of cut (2.5 mm) with a Renishaw NC4+ blue optical tool setter. Fig. 2 shows the experimental layout and equipment within the machine tool.

2. Results

The series of mill-grinding tests resulted in four datasets with a large range in total usable tool life and final DCB wear state. Table 1 shows an overview of the initial and final wear states of each DCB. Due to all parameters being constant between tests, the variance seen in DCB life is the direct result of tool variation or defects.

Table 1. DCB mill-grinding test overviews

Test No.	No. of grinding passes	Material removed (mm^3)	DCB mean radius		
			Initial (mm)	Final (mm)	Wear (%)
1	213	6.39	0.676	0.636	5.91
2	163	4.89	0.662	0.635	4.08
3	176	5.28	0.674	0.610	9.50
4	158	4.74	0.665	0.610	8.27

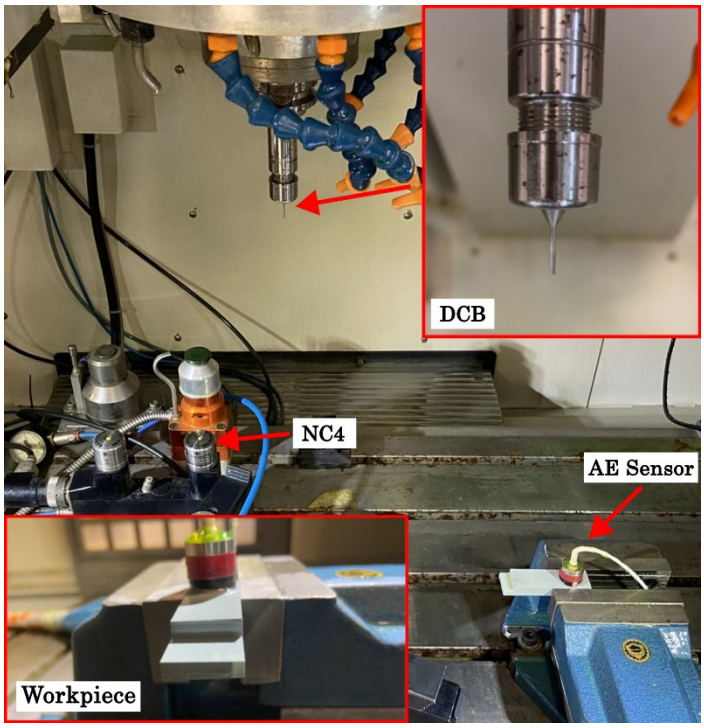

Fig. 2. Labelled experimental layout within machine tool

2.1 DCB Wear Data

After each test, the NC4 surface scans were aligned to show the degradation of the tool's surface during each mill-grinding test. Fig. 3 shows the DCB circumferential surface measurements throughout Test 4. A large crater can be seen forming in Fig. 3, this crater slowly widens until it encompasses two thirds of the circumference.

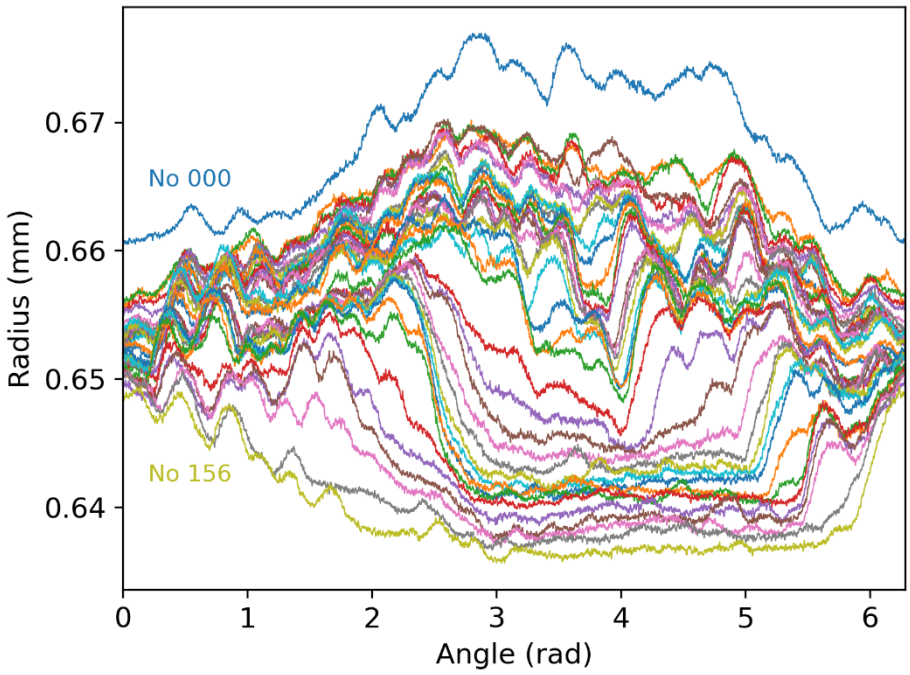

Fig. 3. DCB circumferential surface measurements during Test 4, every fourth measurement shown

To be used as an objective for the AE monitoring procedure, the NC4 tool scans were processed into representative features. Four features were used as the basis for implying the tool's condition, namely; mean radius, peak radius, runout and form error. Mean radius is seen as a generic metric for the DCB's RUL, based solely on the remaining thickness of the abrasive layer. The other three metrics, peak radius, runout and form error, were all utilised as tool condition and effectiveness measurements.

Form error is calculated as the range of each NC4 surface measurement, y_i, seen in equation 1. As a result it indicates the difference in height between the peaks and troughs present on the tool's surface.

$$FormError_i = \max(y_i) - \min(y_i) \quad (1)$$

Runout is a measure of the geometric deviation of the measured surface, from the theoretical rotation axis of the spindle. Multiple sources of runout exist between components within the machine tool, i.e. the machine spindle, tool holder, collet, tool shaft and mean grain surface. Runout is prevalent in all forms of machining, but becomes crucial when using smaller diameter tools making small depth of cuts. Runout is calculated by taking the centre coordinates, (x_0, y_0), of a least squares fitted circle to the measured surface plot, and then finding the distance between the fitted centre and theoretical centre. Equation 2 shows the calculation of total runout from the centre of each tool's fitted centre.

$$Runout_i = 2 \times \sqrt{x_0^2 + y_0^2} \quad (2)$$

Fig. 4 shows the extracted DCB wear features for each of the four tests. Both the mean and peak radius measurements follow the expected three phase wear cycle of grinding tool wear. Runout and form error are both identifiers of surface crater formation, represented by large increases in the measurements after inflection points.

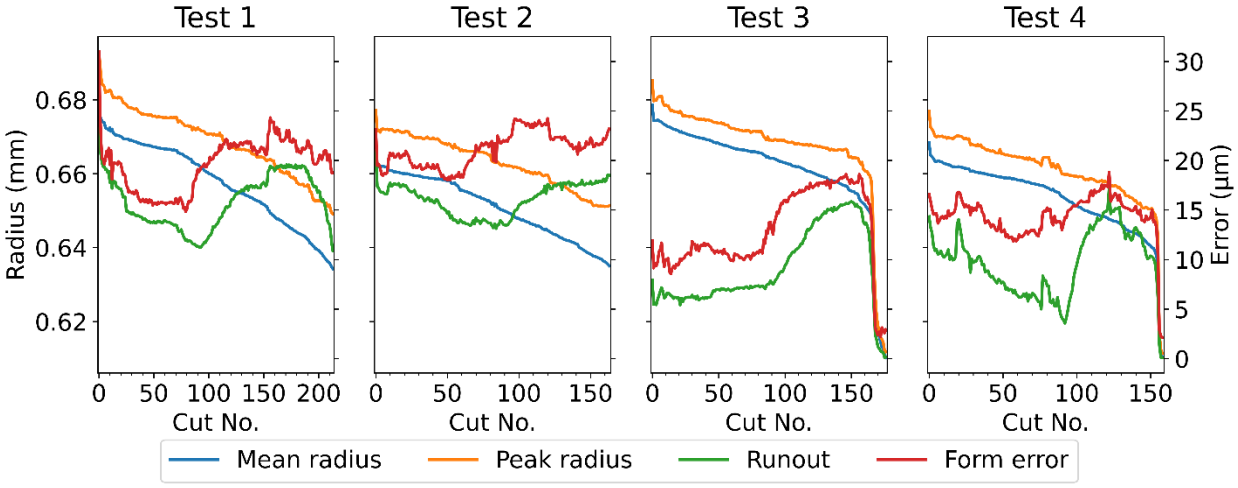

Fig. 4. DCB measurements extracted from NC4 scans during each mill-grinding test

2.2 AE Data

Fig. 5(a) shows a typical AE signal collected during a grinding cut. To ensure reliable capture of the entire AE waveform, an adequate acquisition buffer is added to either side of the grinding. The period of grinding can clearly be identified within the continuous AE signal by sharp increase in amplitude over the 21 s period. To prevent the external noise during these buffer periods impacting the extracted AE features, each signal was trimmed between two trigger points, marked by red dashed lines in figure Fig. 5(a).

Fig. 5(b) shows the same AE signal zoomed into a section lasting 50 ms, better showing the interrupted nature of the grinding process.

To calculate the trigger points for each AE signal automatically, a process based on the gradient of the instantaneous analytical signal from the Hilbert transform was utilised, Fig. 6 shows the process. To further speed up computation time and reliability, the enveloped signal was only computed over the first 5 s in order to determine the trigger start and voltage values. Fig. 7 shows the output of this process for the AE signal shown in Fig. 5.

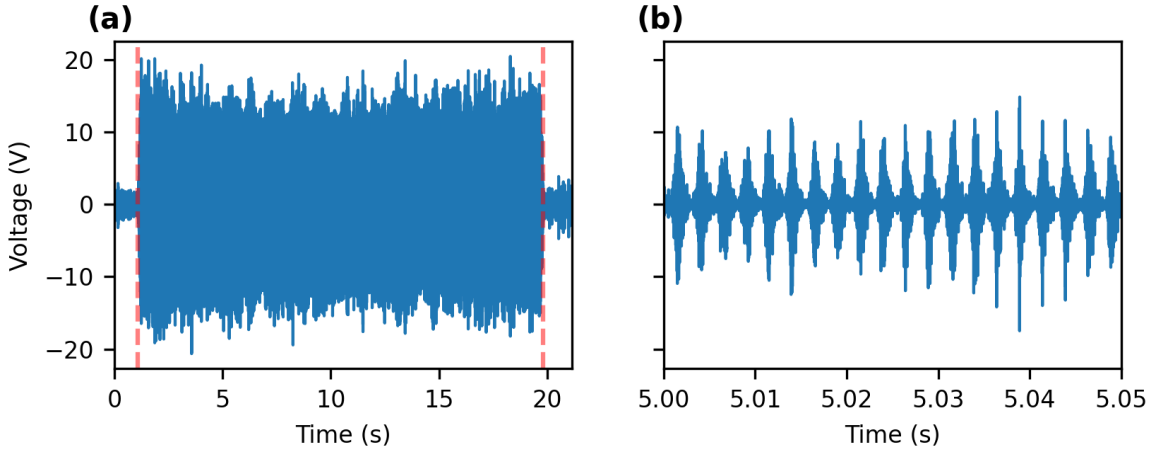

Fig. 5. (a) AE signal from the 10th cut of Test 1, with trigger points shown by red dashed line. **(b)** Zoomed section showing individual AE peaks

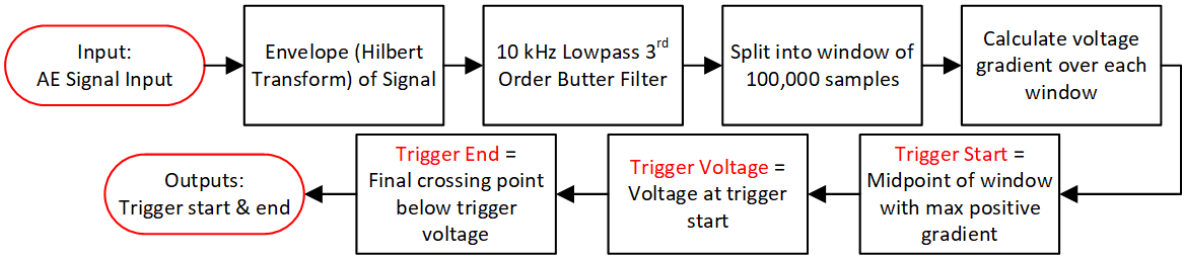

Fig. 6. Flowchart of trigger point determination process

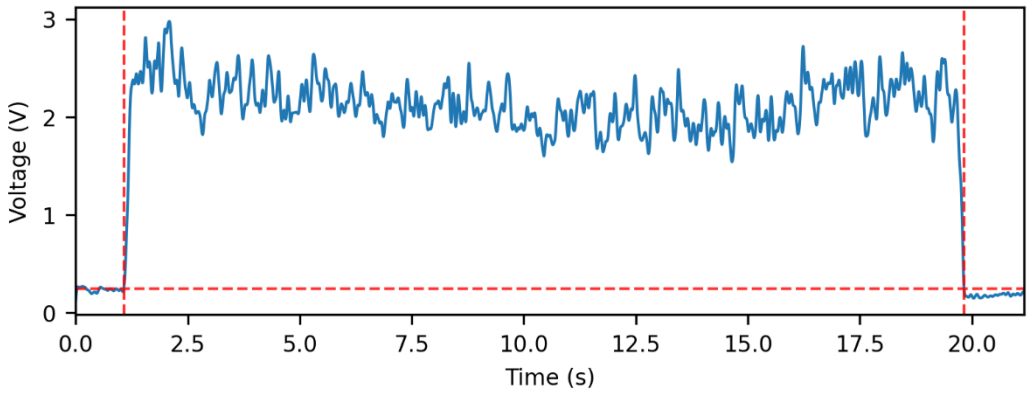

Fig. 7. Filtered and enveloped AE signal with trigger points shown, of the 10th cut of Test 1

Utilising these trigger points, AE features could be extracted relating solely to the period of grinding. Of the time domain features the AE kurtosis (AE_{kurt}) showed the most promise to enable tool state characterisation.

The AE_{kurt} of each signal appeared to be intrinsically linked to the DCB form error and runout. The kurtosis of a signal describes the tailedness of a distribution, which in this application of continuous noise, indicates the proportion of the signal having been measured

at zero voltage. If the grinding tool is assumed to be perfectly circular and have zero runout, it should produce a constant uninterrupted AE signal. However, as can be seen in Fig. 5(b) this is not the case, with the AE amplitude fluctuating at a frequency equal to the spindle speed, 24000 rpm. Suggesting that the tool is only grinding on one section of its circumference, as a result of uneven grit distribution or loss of contact with the workpiece. As such the AE_{kurt} can be seen as a measure of the amount of grinding contact the tool has with the workpiece over one rotation, i.e. an increase in AE_{kurt} implies a loss of contact. Interrupted contact can be the combined result of both DCB runout and form error as well as the overall total wear of the tool.

Fig. 8 shows the corresponding AE_{kurt} and DCB tool errors throughout each of the four mill-grinding tests, in which changes in runout and form error are often accompanied by changes in AE_{kurt}. Examples of this can be seen within all four tests shown in Fig. 8. In Test 1 however, the AE_{kurt} inflection point occurs at cut 60, roughly 20 cuts prior to it being detected within the DCB runout or form error measurements. This example shows a limitation of this experimental method, as the NC4 tool measurements occur only at one circumferential height up the tools contact surface. As a result it is possible, that outside of the measurement region the tool has experienced a change in runout or form error, causing the change in AE_{kurt}. These tests indicate the suitability of AE_{kurt} for the identification of surface crater formation. With this added information relating to each tool's condition, more sophisticated TCM approaches can be developed. Approaches that not only predict tool failure, thus extending each DCB's RUL, but also prevent the usage of a tool that is ineffective and damaging to the workpiece's surface.

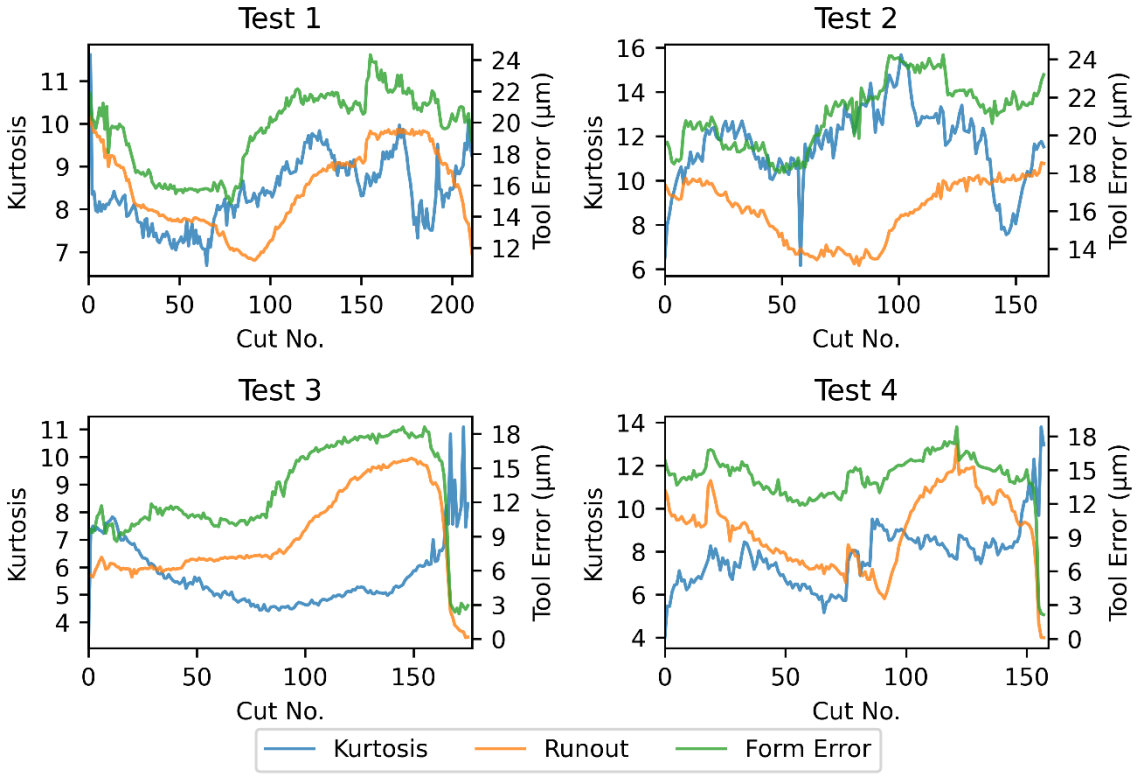

Fig. 8. AE_{kurt} throughout each mill-grinding test with corresponding DCB runout and form error

Looking forward, this work will investigate the effect of tool wear on the workpiece, particularly the effect of surface craters and high runout levels. With the aim of extracting tool wear limits based not solely on tool radius, but also on workpiece tolerances and surface

quality. Additionally, a method of visualising the entire tool's contact surface would give better representation of the tool to relate to the AE signals.

4. Conclusion

This study details the experimental and post-processing methodology for the acquisition of both continuous AE data and in-machine tool wear measurements, during a DCB mill-grinding test. Four full length mill-grinding tests were conducted with constant grinding parameters, in which a ⌀ 1.3mm #1000 DCB was used from new to failure. In situ tool wear measurements with a Renishaw NC4+ blue, showed the DCBs follow a traditional three phase wear cycle. They also identified the formation of surface craters in each test, resulting in sharp increases in both tool runout and form error. AE feature extraction was aided by the inclusion of trigger points, identifying both the start and end of grinding contact within continuous AE signals. AE_{kurt} presents as a metric for the proportion of circumferential contact between the DCB and workpiece. In turn enabling the identification of surface crater formation on the tools, shown by a correlation between changes in AE_{kurt} and DCB runout and form error. This relationship could enable more traditional overall wear prediction models, commonly based on AE amplitude and frequency partial powers, to better understand the tool's condition and grinding effectiveness.

Acknowledgements

This work was funded by an EPSRC ICASE award in partnership with Renishaw plc. The authors have no competing interests to declare that are relevant to the content of this article.

References

[1] Y. Li, C. Liu, J. Hua, J. Gao, and P. Maropoulos, "A novel method for accurately monitoring and predicting tool wear under varying cutting conditions based on meta-learning," CIRP Annals, vol. 68, no. 1, pp. 487–490, Jan. 1, 2019, ISSN: 0007-8506. DOI: 10.1016/j.cirp.2019.03.010.

[2] S. Kurada and C. Bradley, "A review of machine vision sensors for tool condition monitoring," Computers in Industry, vol. 34, no. 1, pp. 55–72, Oct. 1, 1997, ISSN: 0166-3615. DOI: 10.1016/S0166-3615(96)00075-9.

[3] K. Fathima, A. Senthil Kumar, M. Rahman, and H. S. Lim, "A study on wear mechanism and wear reduction strategies in grinding wheels used for ELID grinding," Wear, vol. 254, no. 12, pp. 1247–1255, Nov. 1, 2003, ISSN: 0043-1648. DOI: 10.1016/S0043-1648(03)00078-4.

[4] B. Azarhoushang and A. Daneshi, "13 - Mechanisms of tool wear," in Tribology and Fundamentals of Abrasive Machining Processes (Third Edition), B. Azarhoushang, I. D. Marinescu, W. Brian Rowe, B. Dimitrov, and H. Ohmori, Eds., William Andrew Publishing, Jan. 1, 2022, pp. 539–554, ISBN: 978-0-12-823777-9. DOI: 10.1016/B978-0-12-823777-9.00020-3.

[5] Z. Li, R. Liu, and D. Wu, "Data-driven smart manufacturing: Tool wear monitoring with audio signals and machine learning," Journal of Manufacturing Processes, vol. 48, pp. 66–76, Dec. 1, 2019, ISSN:1526-6125. DOI: 10.1016/j.jmapro.2019.10.020.

[6] D. F. G. Moia, I. H. Thomazella, P. R. Aguiar, E. C. Bianchi, C. H. R. Martins, and M. Marchi, "Tool condition monitoring of aluminum oxide grinding wheel in dressing operation using acoustic emission and neural networks," Journal of the Brazilian Society of Mechanical Sciences and Engineering, vol. 37, no. 2, pp. 627–640, Mar. 1, 2015, ISSN: 1806-3691. DOI: 10.1007/s40430-014-0191-6.

[7] B. Denkena, J. Jacobsen, and N. Kramer, "Dressing Monitoring by Acoustic Emission," Key Engineering Materials, vol. 291–292, pp. 195–200, 2005, ISSN: 1662-9795. DOI: 10.4028/www.scientific.net/KEM.291-292.195.

[8] C.-S. Liu and Y.-A. Li, “Evaluation of grinding wheel loading phenomena by using acoustic emission signals,” The International Journal of Advanced Manufacturing Technology, vol. 99, no. 5, pp. 1109–1117, Nov. 1, 2018, ISSN: 1433-3015. DOI: 10.1007/s00170-018-2513-9.
[9] C.-S. Liu and Y.-J. Ou, “Grinding Wheel Loading Evaluation by Using Acoustic Emission Signals and Digital Image Processing,” Sensors, vol. 20, no. 15, p. 4092, 15 Jan. 2020, ISSN: 1424-8220. DOI: 10.3390/s20154092.
[10] Z. Wang, P. Willett, P. R. DeAguiar, and J. Webster, “Neural network detection of grinding burn from acoustic emission,” International Journal of Machine Tools and Manufacture, vol. 41, no. 2, pp. 283–309, Jan. 1, 2001, ISSN: 0890-6955. DOI: 10.1016/S0890-6955(00)00057-2.
[11] I. Yesilyurt, A. Dalkiran, O. Yesil, and O. Mustak, “Scalogram-Based Instantaneous Features of Acoustic Emission in Grinding Burn Detection,” Journal of Dynamics, Monitoring and Diagnostics, vol. 1, no. 1, pp. 19–28, 1 2022, ISSN: 2831-5308. DOI: 10.37965/jdmd.2021.49.
[12] D. A. Dornfeld, Y. Lee, and A. Chang, “Monitoring of ultraprecision machining processes,” The International Journal of Advanced Manufacturing Technology, vol. 21, no. 8, pp. 571–578, 2003, ISSN:1433-3015.
[13] X. Han and T.Wu, “Analysis of acoustic emission in precision and high-efficiency grinding technology,” The International Journal of Advanced Manufacturing Technology, vol. 67, no. 9, pp. 1997–2006, Aug. 1, 2013, ISSN: 1433-3015. DOI: 10.1007/s00170-012-4626-x.
[14] M. Shah, V. Vakharia, R. Chaudhari, J. Vora, D. Y. Pimenov, and K. Giasin, “Tool wear prediction in face milling of stainless steel using singular generative adversarial network and LSTM deep learning models,” The International Journal of Advanced Manufacturing Technology, vol. 121, no. 1, pp. 723–736, Jul. 1, 2022, ISSN: 1433-3015. DOI: 10.1007/s00170-022-09356-0.
[15] R. E. Haber, J. E. Jimenez, C. R. Peres, and J. R. Alique, “An investigation of tool-wear monitoring in a high-speed machining process,” Sensors and Actuators A: Physical, vol. 116, no. 3, pp. 539–545, Oct. 29, 2004, ISSN: 0924-4247. DOI: 10.1016/j.sna.2004.05.017.
[16] G. Bi, S. Liu, S. Su, and Z. Wang, “Diamond Grinding Wheel Condition Monitoring Based on Acoustic Emission Signals,” Sensors, vol. 21, no. 4, 2021, ISSN: 1424-8220. DOI: 10.3390/s21041054.
[17] L.Wan, X. Zhang, Q. Zhou, D.Wen, and X. Ran, “Acoustic emission identification of wheel wear states in engineering ceramic grinding based on parameter-adaptive VMD,” Ceramics International, vol. 49, pp. 13 618–13 630, 9, Part A May 1, 2023, ISSN: 0272-8842. DOI: 10.1016/j.ceramint.2022.12.238.
[18] G. Bi, S. Zheng, and L. Zhou, “Online monitoring of diamond grinding wheel wear based on linear discriminant analysis,” The International Journal of Advanced Manufacturing Technology, vol. 115, no. 7, pp. 2111–2124, Aug. 1, 2021, ISSN: 1433-3015. DOI: 10.1007/s00170-021-07190-4.
[19] B.-S. Wan, M.-C. Lu, and S.-J. Chiou, “Analysis of Spindle AE Signals and Development of AE-Based Tool Wear Monitoring System in Micro-Milling,” Journal of Manufacturing and Materials Processing, vol. 6, no. 2, p. 42, 2 Apr. 2022, ISSN: 2504-4494. DOI: 10.3390/jmmp6020042.
[20] H. Murakami, A. Katsuki, T. Sajima, K. Uchiyama, K. Houda, and Y. Sugihara, “Spindle with built-in acoustic emission sensor to realize contact detection,” Precision Engineering, vol. 70, pp. 26–33, Jul. 1, 2021, ISSN: 0141-6359. DOI: 10.1016/j.precisioneng.2021.01.017.
[21] W. B. Rowe, X. Chen, and D. R. Allanson, “The Coolant Coupling Method Applied to Touch Dressing in High Frequency Internal Grinding,” in Proceedings of the Thirty-Second International Matador Conference, A. K. Kochhar et al., Eds., London: Macmillan Education UK, 1997, pp. 337–340, ISBN: 978-1-349-14620-8. DOI: 10.1007/978-1-349-14620-8_53.
[22] I. Inasaki, “Application of acoustic emission sensor for monitoring machining processes,” Ultrasonics, Ultrasonics International 1997, vol. 36, no. 1, pp. 273–281, Feb. 1, 1998, ISSN: 0041-624X. DOI: 10.1016/S0041-624X(97)00052-8.
[23] Renishaw plc. “Renishaw: NC4,” Renishaw. (), [Online]. Available: http://www.renishaw.com/en/high-accuracy-laser-tool-setting-systems--6099.
[24] Y. Wang, J. Xiang, R. Markert, and M. Liang, “Spectral kurtosis for fault detection, diagnosis and prognostics of rotating machines: A review with applications,” Mechanical Systems and Signal Processing, vol. 66–67, pp. 679–698, Jan. 1, 2016, ISSN: 0888-3270. DOI: 10.1016/j.ymssp.2015.04.039.
[25] T. Jessel, C. Byrne, M. Eaton, B. Merrifield, S. Harris, and R. Pullin, “Tool condition monitoring of diamond-coated burrs with acoustic emission utilising machine learning methods,” The International Journal of Advanced Manufacturing Technology, vol. 130, no. 3, pp. 1107–1124, Jan. 1, 2024, DOI: https://doi.org/10.1007/s00170-023-12700-7.